CrossMark

Punching Shear Failure of Concrete Ground Supported Slab

Oldrich Sucharda[1],* , Martina Smirakova[2] , Jana Vaskova[2] ,
Pavlina Mateckova[2] , Jan Kubosek[2] , and Radim Cajka[2]

Abstract: The article handles potential approaches to design and determination of total load capacity of foundation slabs and floors. The research is focused on punching shear failure of reinforced ground supported slab. The article presents detailed results of the experiment made and advanced numerical modelling based on nonlinear analysis and application of fracture-plastic model. The experiment made included a 2.0×1.95 m reinforced concrete slab-on-ground of 120 mm thickness. The experiment was followed by a parametric study of total load capacity calculation with nonlinear analysis which is supplemented by calculations based on existing design model code.

Keywords: punching shear analysis, concrete slab, ground-supported slab, reinforced, fracture-plastic model, nonlinear analysis, fracture-plastic material.

1. Introduction

The punching shear resistance of reinforced concrete ground supported slab represents a wide category of concrete structure and subsoil interaction problems. The spatial fracture mechanism itself is influenced by various input parameters. The most important ones include geometrical dimensions of the structure, properties of the selected concrete materials, load or properties and characters of soil underneath. The importance of this research area is testified by the extensive research underway—see Kueres et al. (2017), Hoang and Pop (2016), Alani and Beckett (2013), Halvonik and Fillo (2013), Siburg et al. (2012), Siburg and Hegger (2014), Song et al. (2012), and Husain et al. (2017). General evaluation of tests of typical slabs is provided in Alani and Beckett (2013) and Ricker and Siburg (2016). An interesting comparison and critical review of the punching shear strength of flat slabs can be found in Bogdándy and Hegedus (2016) or Zabulionis et al. (2006). Important overall results from the field of behaviour of reinforced concrete footings are presented also in Siburg and Hegger (2014), Hegger et al. (2006, 2007), Aboutalebi et al. (2014) and Siburg et al. (2014). The approaches to calculation, modelling and computer programs are focused on in Kotsovou et al. (2016), Ibrahim and Metwally (2014), Cajka (2014) and Kolár and Nemec (1989). However, the comparison and description of experiments are based most commonly on traditional approach to reinforced concrete structure designing.

Because of complexity of the task the design models are prepared attempting to appropriately simplify the issue or applying many limitations. This enables to obtain the required design criteria and provide safety for the selected cases. Due to the simplification, the results of the applied calculation models are applicable only to the specific cases. The result value for atypical and nonstandard configurations is limited or remarkably distorted. Typical cases include concrete slabs with low thickness, high load or as well as applications of new composite materials (Sucharda et al. 2017).

The design codes for this area already known include ACI 318-08 (2008), Norm SIA 262 (2003) and EC2 (2006) which is based on Model Code 1990 (1993) and in which case it should be noted that there is also Model Code 2010 (2012). This recommendation enables to use the typical approaches mentioned above for the design as well as application of advanced calculation simulations which reflect also the real concrete behaviour. The application of simulations themselves enables, in particular, to cover specific construction and design cases.

Because of the aforementioned extensive research and specifics in this concrete application area there is still a space for research. The research is focused on optimization of design and material of concrete slabs with low thickness for cases of high load. Typically, the slabs form structures and floors in heavy industry and ground of aircraft taxiing areas. The need of research is generated especially by requirements of practical application because VŠB-Technical University

[1]Department of Building Materials and Diagnostics of Structures, Faculty of Civil Engineering, VŠB-Technical University of Ostrava, Ludvíka Podéště 1875/17, 708 33 Ostrava-Poruba, Czech Republic.
*Corresponding Author; E-mail: oldrich.sucharda@vsb.cz
[2]Department of Structures, Faculty of Civil Engineering, VŠB-Technical University of Ostrava, Ludvíka Podéště 1875/17, 708 33 Ostrava-Poruba, Czech Republic.

of Ostrava is located in the largest industrial region in the Czech Republic. This region is characteristic by orientation on heavy industry and machine industry where reconstruction or construction projects are being prepared. However, often the typical approach to concrete structure designing using simplified calculation models is not well suited and applicable. For those reasons novel innovative approaches to designing are to be searches for.

2. Research Significance

The article deals with punching shear failure of reinforced concrete slabs with low thickness exposed to high load in interaction with the ground. Its objective is to evaluate the experiment made and the total load capacity of concrete slabs using computer simulations reflecting real behaviour. The concrete slab is provided with reinforcing bars at the lower surface and is centrically loaded. The calculation simulations are supplemented with option calculations based on the current design code EC2. In case of calculation simulations the modelling is based on the approach included in new Model Code 2010 (2012). Spatial calculation models and fracture-plastic concrete models are applied. Considering the task nature and scope the numerical calculations are made in several options which are discussed. This applies particularly to the case of selection of input parameters for concrete and modelling of the slab—ground interaction. The article objectives comprise also verification of the concrete slab failure mode. The calculations and experiment made enable to assess the applicability of numerical models and calculation procedures for determination of total load capacity of concrete slabs.

3. Methodology and Procedures Experiment

3.1 Advanced Numerical Modelling and Nonlinear Analyses

The application of typical verification and design models for concrete structures is a logical and in most cases also a comfort solution. However, there are cases where it is impossible. This applies to, for example, immense new requirements from architects, research of material engineers or simply practical application needs. The general results of research in the field of concrete and concrete structures for the last 20 years are summarized in new Model Code 2010 (2012) recommendation. The Model Code 2010 (2012) recommendation contains the basic principles and procedures for concrete application including the use of advanced numerical modelling and reinforcement concrete nonlinear analyses. The application is referred to also in ASCE (1982) and Barzegar (1988). It should be noted that the recommendation states several possibilities for application of concrete material models in nonlinear analysis. This applies to elastic–plastic models, models based on fracture mechanics (Bazant and Planas 1998) or combined models (Cervenka and Papanikolaou 2008). This basic division is

further developed to specific constitutive concrete models. The popular models include disturbed stress field model for reinforced concrete (Vecchio and Shim 2004) and microplane model (Bazant et al. 2000). For the numerical modelling, the fracture-plastic material model is selected in the research. The material models themselves differ mainly in the number of required input information on the concrete. The compressive strength and modulus of elasticity are insufficient information. Typically it is necessary to determine the concrete tensile strength and fracture-mechanical parameters where the basis for their determination can be found also in Model Code 2010 (2012). Certain information is provided also in ISO 2394 (1998) and JCSS (2016). The determination of material parameters are subject of many research projects. A particularly difficult task is to determine the concrete tensile strength (Sarfarazi et al. 2016). The results often show high spread of measured data. The latest advanced methods include identification of material properties combining laboratory tests and inversion analyses with computers modelling using sophisticated algorithms. The methods comprise stochastic modelling, application of neuron networks, multiple-criteria decision analysis, etc.

3.2 Description of Punching Shear Failure
Punching shear failure is one of the typical concrete slab collapses. Punching shear may result from a concentrated load or reaction acting on a relatively small area. For ease of reference, the following description of the task solution is based on the punching failure verification model presented in EC2 (2006)—see Fig. 1.

This area is called the loaded area, A_{load}, of a slab or foundation. The shear resistance should be checked along control perimeters (at the perimeter of the loaded area u_0 and at the basic control perimeter u_1). In special cases, for example, footings, the load within the control perimeter due to ground pressure adds to the resistance and may be subtracted when determining the design punching shear stress.

The basic control perimeter u_1 may normally be taken to be at a distance $2d$ from the loaded area and should be constructed to minimise its length. The following text will concentrate on the square cross-section because the loaded area at the experiments has a square shape. All equations from EC2 (2006) will then be modified for a foundation slab.

3.3 Test Setup and Measurement
The test setup selection was based on the verification model for punching shear and capabilities of special test frame designed for concrete slab testing. The test slab dimensions were $2000 \times 1950 \times 120$ mm. C16/20 concrete was used for concreting. Hand-fastened Ø8/100 mm reinforcing mesh of B500B steel was inserted in the slab. Shear reinforcing was not performed. Reinforcing and concreting are shown in Figs. 2 and 3. The slab was concreted on layer-compacted gravel with a thickness of 0.3 m from fraction 0/4 mm, which was laid on the original subsoil without greensward. The subsoil characteristics were measured (Lahuta et al. 2015). The original subsoil consisted of
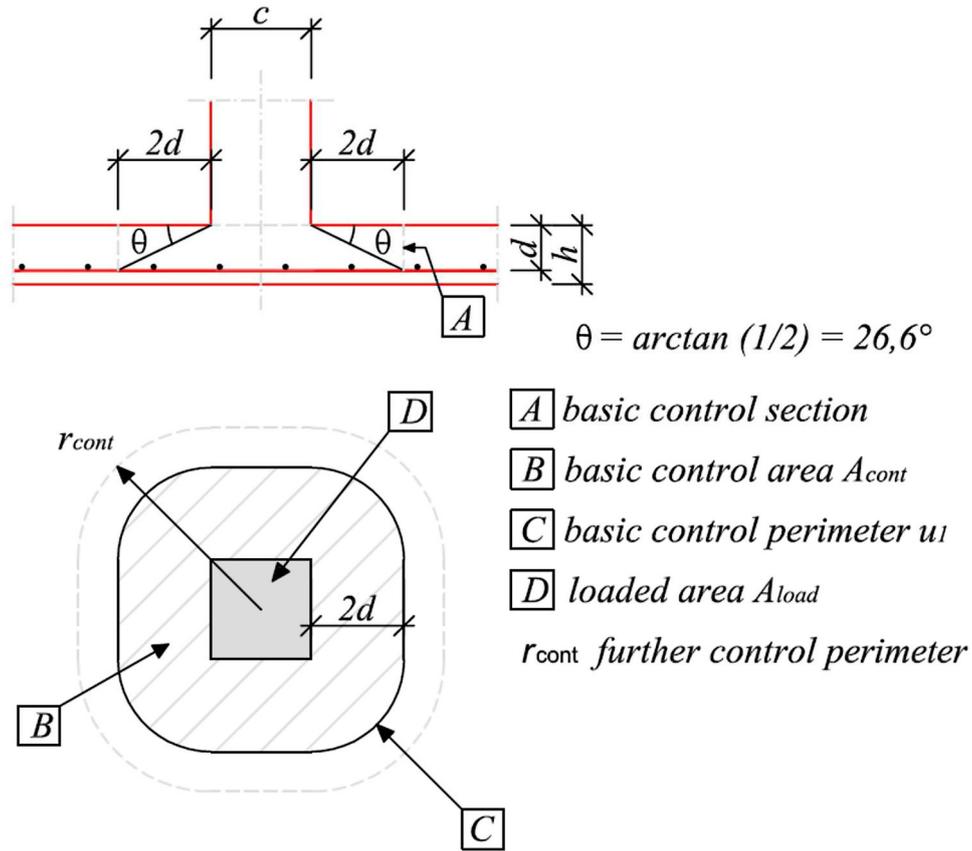
Fig. 1 Verification model for punching shear at the ultimate limit state.

$$\theta = arctan\ (1/2) = 26,6°$$

A basic control section

B basic control area A_{cont}

C basic control perimeter u_1

D loaded area A_{load}
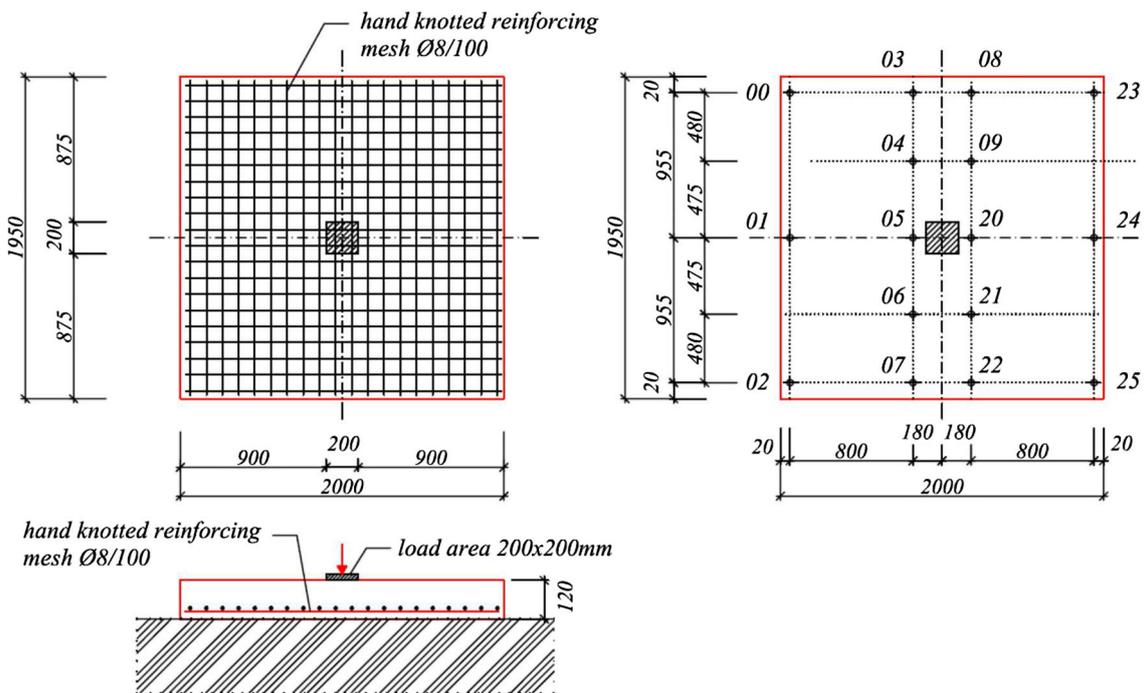
r_{cont} *further control perimeter*

Fig. 2 The test sample and placement of deformation sensors (mm).

loess loam with consistency F4, and its thickness was approximately 5 m. The volumetric weight of the soil was $\gamma = 18.5$ kN m^{-3}, the Poisson coefficient was $\nu = 0.35$ and the static Young's modulus was $E_{def} = 33.86$ MPa. During the experimental loading test, the reinforced concrete slab was loaded by pressure in the centre. The pressure was reached through use of a hydraulic jack (Figs. 2 and 3). The loaded area A_{load} was 200×200 mm.

The test setup included a comprehensive set of measurements. Vertical loading magnitude, vertical settlement and

Fig. 3 Concreting of the slab model and loading test. **a** Concreting of the slab and **b** Loading test

slab deformations were measured. Vertical deformation was measured at 16 points. The sensor positions are shown in Fig. 3. The hydraulic press and sensor set were synchronized using Ahlborn measuring device. Tensometric measurements were also taken at selected points of the concrete slab to verify the slab behaviour.

3.4 Reinforced Concrete Slab Test

A reinforced concrete slab in the configuration described above was exposed to pressure in cycles, and each load step was carried out after a half hour. In each load step, 50 kN was added. The maximum loading force of 344 kN was achieved by the gradual loading. The slab was failed by punching shear. After completion of the loading test, the corrupted slab was lifted, and the progress and width of cracks on the lower surface of the slab were examined. The shape of the failure zone is not symmetrical, even though the shape of the slab, the reinforcement and the load were symmetrical. Cracks on the bottom surface of the foundation can be seen in Fig. 4. The concrete slab is suspended on a rope and is visible from the

slope. The results of vertical slab deformations are illustrated in five loading cycles (150, 200, 250, 300 and 344 kN) for four slab cross-sections in vertical direction in Fig. 5 and in three horizontal directions in Fig. 6. The deformations indicate that higher load intensities led to uneven settlement. This can be caused by the subsoil and progress of the concrete failure on one slab side. The failure is detailed and discussed below.

3.5 Punching Shear Resistance and Failure of the Tested Slab

In Fig. 7, the real shape of the crack on the upper surface of the slab is drawn by the pink curve. According to the shape of the crack, there is apparent failure of the slab caused by punching shear.

The crack, marked by the pink curve, corresponds to the edge of the loaded area A_{load}. The theoretical verification model of the ultimate limit state for punching failure (according to EC2 2006) is transferred to the photography of the concrete slab model. Figure 7 shows the loaded area (D), which represents the loaded area edge (pink curve) and the
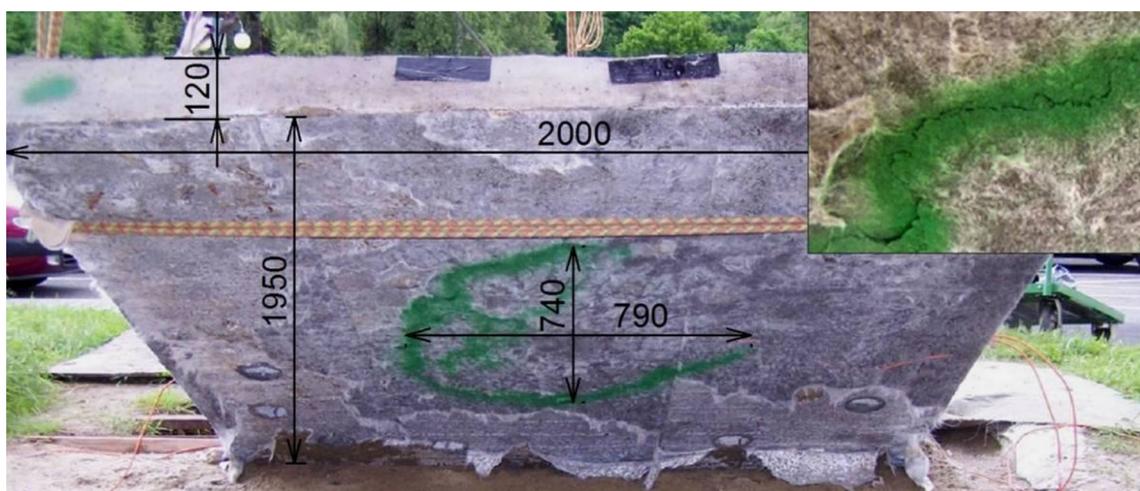

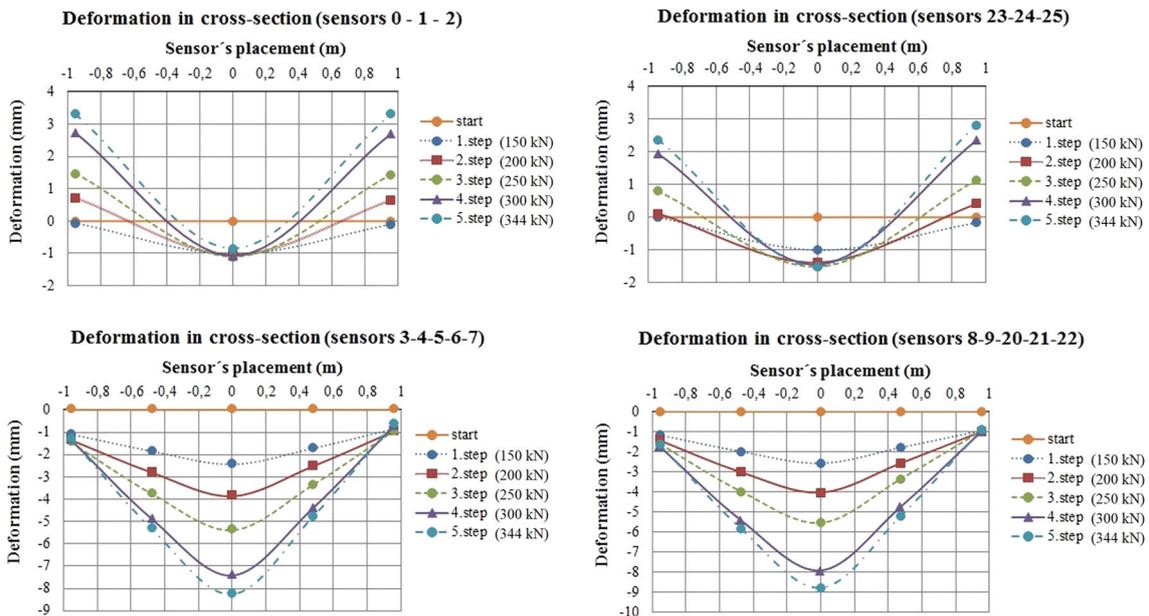**Fig. 4** Cracks on the bottom surface of the slab (mm).

Fig. 5 Vertical deformation of the slab—in cross-sections (mm).
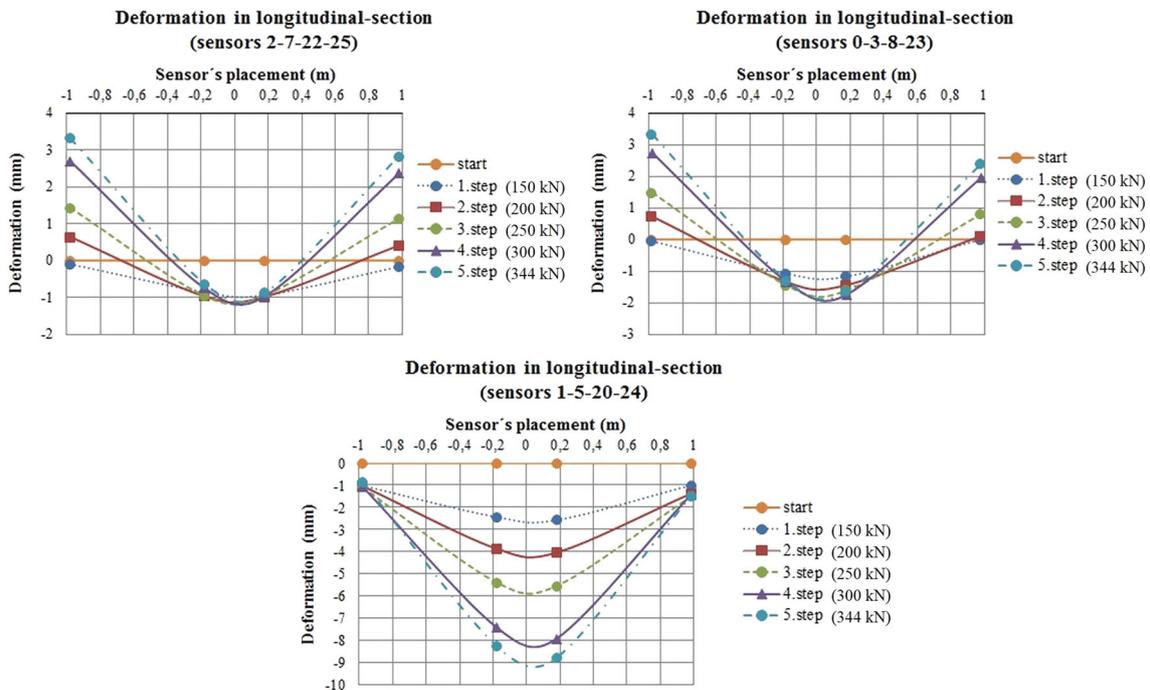

Fig. 6 Vertical deformation of the slab—in longitudinal-sections (mm).

theoretical basic control perimeter (C) at the distance 2*d* from the loaded area edge (blue dotted curve).

The theoretical basic control perimeter (C) is located at the level of the reinforcement. Real cracks in the level of reinforcement of the loaded slab model are marked with the orange dashed curve (B).

The theoretical control perimeter (C) was compared with a perimeter illustrating the real shape of cracks incurred on the loaded slab model (B). In Fig. 7, there is also drawn an approximate of the real shape of the cracks on the bottom surface of the concrete slab (yellow dashed curve). These cracks are also shown in the photo in Fig. 4. The failed slab was cut in eight cuts, transversely and diagonally. These

individual cuts are numbered in Fig. 7. In Figs. 8 and 9, eight cuts in the slab are viewed. Cut numbers 1–4 are guided laterally, and cut numbers 5–8 are guided diagonally (see Fig. 7). The real shape and slope of the cracks in the cut is pink. The approximate slope of the crack is marked with a yellow dashed line. The crack spreads from the top surface of the slab and the loaded area edge through the cross-section to the reinforcement and the lower plate surface. The real dimensions measured during the load test are depicted in black, and the blue dotted dimension represents the theoretical values (*d*, 2 *d*, θ angle) indicated in the verification model of the ultimate limit state for punching failure (according to EC2 2006, Fig. 1). In the pictures of all of the
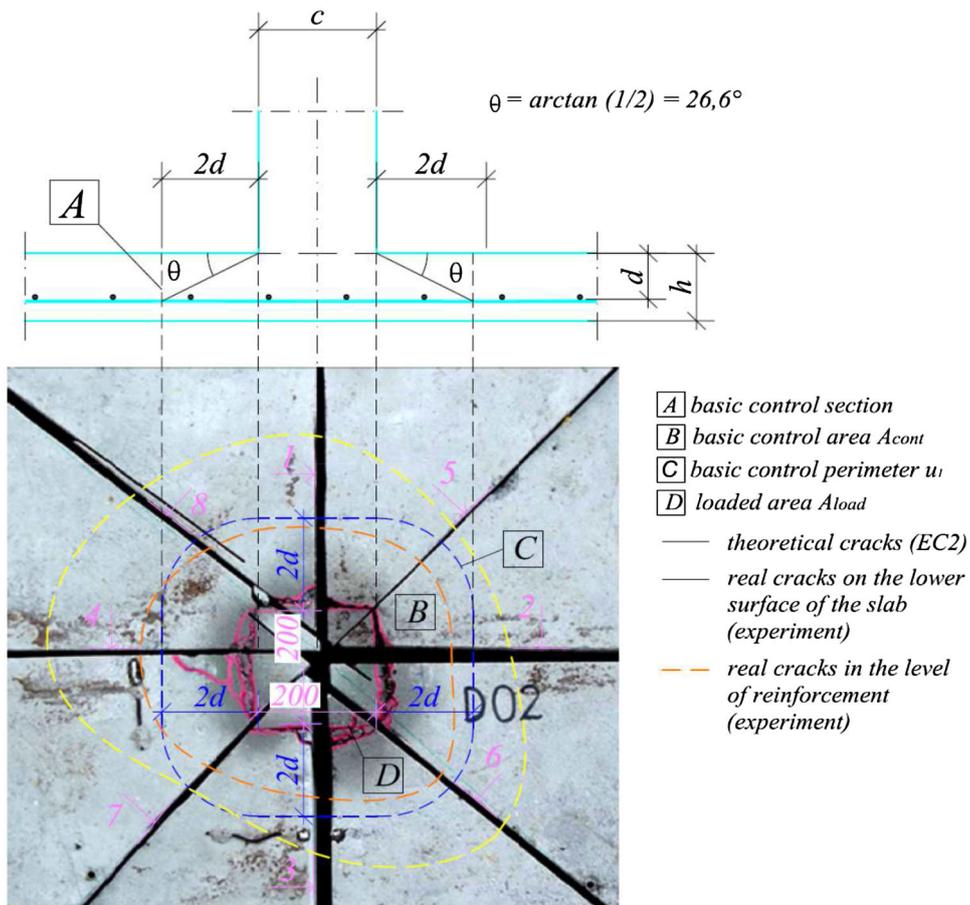
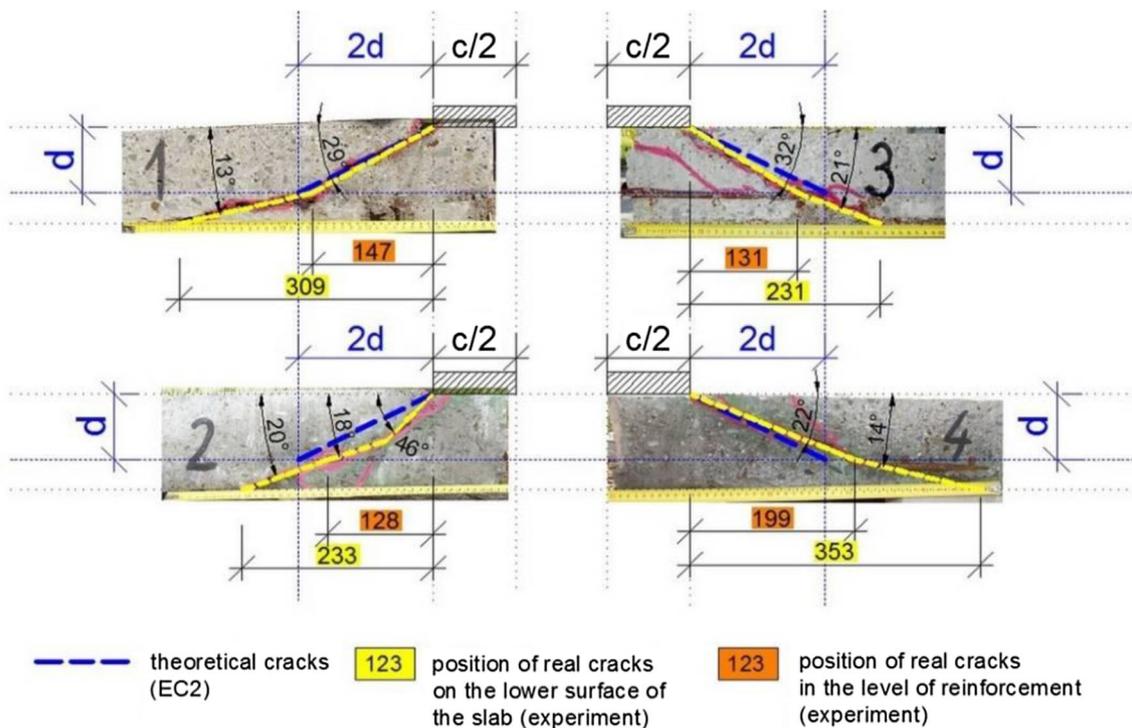**Fig. 7** Verification model for punching shear at the ultimate limit state (mm).

Fig. 8 Comparison of the measured values and the results of the design methods used in EC2 in lateral cuts of the slab (mm).
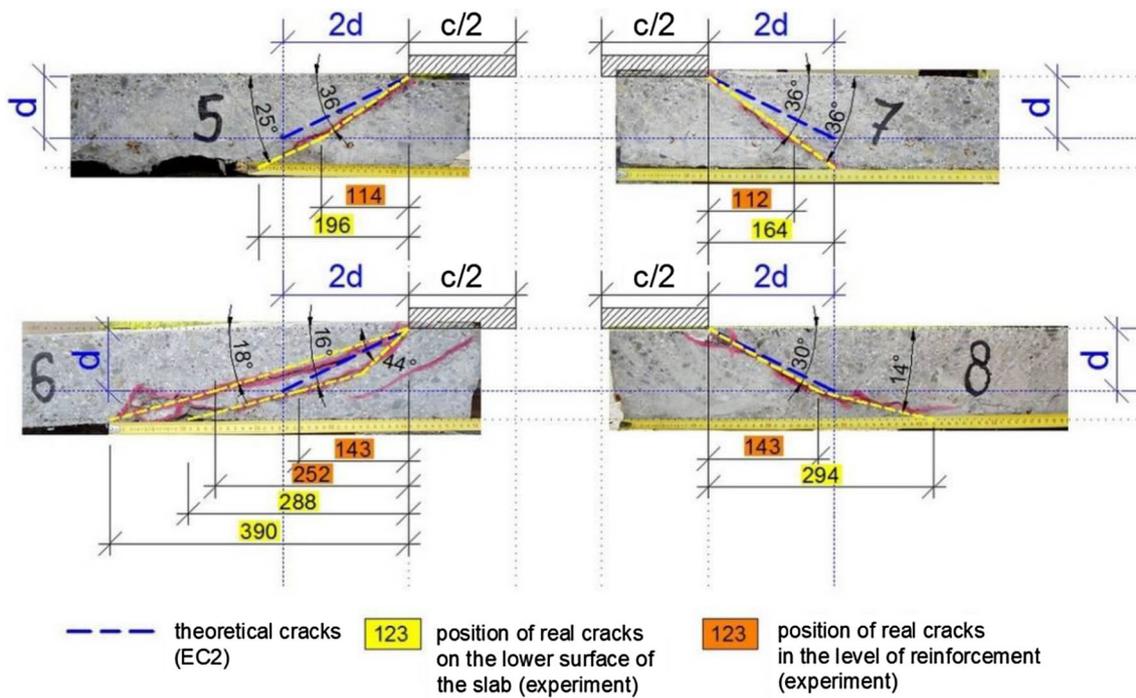
Fig. 9 Comparison of the measured values and the results of the design methods used in EC2 in diagonal cuts of the slab (mm).

Table 1 Evaluation of real location of the crack.

Section number	Values relative to the level of reinforcement				Values relative to the level of the lower surface of the slab		
	Distance of the crack from the centre of the loaded area (mm)	Distance of the crack from the loaded area (mm)	Ratio d	Angle of inclination (°)	Distance of the crack from the centre of the loaded area (mm)	Distance of the crack from the loaded area (mm)	Angle of inclination (°)
1	247	147	1.79	29.01	409	309	13.20
2	228	128	1.56	32.39	333	233	19.88
3	231	131	1.60	31.81	331	231	20.78
4	299	199	2.43	22.36	453	353	13.86
5	254	114	1.39	35.32	336	196	24.80
6	283	143	1.74	29.67	428	288	14.68
7	252	112	1.37	35.77	304	164	35.73
8	283	143	1.74	29.67	434	294	14.12
Average value	259.63	139.63	1.70	30.75	378.50	258.50	19.63
Determinative deviation s	24.27	25.57	0.31	3.96	54.42	59.01	7.22
Variation range R	71.00	87.00	1.06	13.42	149.00	189.00	22.53

cuts, the slab thickness h and half of the loaded area $c/2$, which shows the distance from the loaded area edge and middle of the slab, are indicated.

The theoretical slope is indicated by the angle according to the model of EC2 (2006) (blue dotted line). This slope is guided from the loaded area edge to a distance of 2d (blue dotted line), where d is the distance between the top surface and reinforcement (blue dotted line). In Figs. 8 and 9, the

real slopes of the crack are also marked. The real distances of the crack from the slab centre at the level of reinforcement (highlighted in orange) and on the lower surface of the slab (highlighted in yellow) are also marked in Figs. 8 and 9.

The distances are between 112 mm and 199 mm and are similar to the value of EC2 (2006). Evaluation of these values is given in Table 1. From Table 1 it is clear that the value of the critical perimeter is not 2d as in Eurocode but

about 1.7 d. If such distributions would have more input parameters, those could be then used as input parameter to probability assessment of structure.

4. Calculation of Load Capacity of Tested Slab

4.1 Load Capacity of Tested Slab According to EC2

In case of the selected concrete slab test configuration the main factor for the total load capacity determination is the punching shear failure. The slab load capacity was determined based on the above mentioned approach included in EC2 (2006). Punching shear may be the result of a concentrated load or reaction acting on a relatively small area. This area is called the loaded area A_{load} of a slab or foundation. For checking punching failure at the ultimate limit state, a verification model is given in EC2 (Fig. 1). The shear resistance should be checked along control perimeters. In special cases, for example, footings, the load within the control perimeter adds to the resistance of the structural system and may be subtracted when determining the design punching shear stress. Shear resistance of a slab was verified according to (EC2) for slabs without shear reinforcement and with the influence of the subsoil. The design of punching shear stress is then given by:

$$v_{Rd,c} = C_{Rd,c} \cdot k \cdot (100 \cdot \rho_1 f_{ck})^{\frac{1}{3}} \cdot 2d/a \geq v_{min} \quad 2d/a \quad (1)$$

where f_{ck} is the concrete compressive strength (MPa) and a is the distance from the periphery of the column to the control perimeter considered $\langle 0.5d \leq a \leq 2d \rangle$. The other coefficients are expressed as:

$$k = 1 + \sqrt{\frac{200}{d}} \leq 2,0 \quad (2)$$

and

$$\rho_1 = \sqrt{\rho_{1y} \cdot \rho_{1z}} \leq 0,02 \quad (3)$$

where ρ_{1y} and ρ_{1z} relate to the bonded tension steel in y- and z- direction, respectively.

The value of $C_{Rd,c}$ and v_{min} for use in a country may be found in its National Annex and the calculation k gives the Eq. (2). The recommended value show according to the Czech National Annex for $C_{Rd,c}$. The punching resistance of column bases should be verified at control perimeters within 2.0 d from the periphery of the column. The lowest value of ratio punching resistance/shear force defined position of critical control perimeter.

For axis-symmetric loading, the net applied force is:

$$V_{Ed,red} = V_{Ed} - \Delta V_{Ed} \quad (4)$$

where V_{Ed} is the column load; ΔV_{Ed} is the net upward force within the control perimeter considered, i.e., upward pressure from soil minus self-weight of base.

Then, shear stress is

$$v_{Ed,i} = \frac{V_{Ed,red}}{u_i \cdot d} \quad (5)$$

The above equations were used to calculate the maximum applied force V_{Ed} that causes punching shear failure. From (4) and (5), $V_{Ed,i}$ can be derived:

$$v_{Ed,i} = \frac{V_{Ed,red}}{u_i \cdot d} = \frac{\sigma \cdot A^*}{u_i \cdot d} = \frac{\frac{V_{Ed,press}}{A_{pl}} \cdot (A_{pl} - A_i)}{u_i \cdot d} \quad (6)$$

where σ is contact stress in the foundation bottom; $V_{Ed,press}$ is applied force; A_{pl} is area of the whole slab (or of contact area); A_i is basic control area.

If $v_{Ed,i} = v_{Rd,i}$, then $V_{Ed,press,i}$ in that particular perimeter will be

$$V_{Ed,press,i} = \frac{A_{pl} \cdot v_{Rd} \cdot u_i \cdot d}{(A_{pl} - A_i)} \quad (7)$$

The value of the applied force that causes slab failure can be for $a = 2d$ and Table 2 (standard values) calculated using Eq. (7):

$$V_{Ed,press,i} = \frac{A_{pl} \cdot v_{Rd} \cdot u_i \cdot d}{(A_{pl} - A_i)} = 60.13 \, \text{kN} \quad (8)$$

By the same process, other forces in other perimeters can be calculated. The punching shear resistance of the foundation slab in other perimeters (from perimeter of loaded area to critical perimeter 2 d, which means a = $\langle 0.5d; 2d \rangle$) is shown in Fig. 10. Theoretical values of the applied force $V_{Ed,i}$, which causes slab failure, are presented in Table 2. Different values of $V_{Ed,i}$ are presented according to the used capacity of concrete. Average values of capacity f_m were used in the test on the same day as the experiment, then 5% quantile from the measured values were used. The last value of punching shear resistance was calculated from the tabular strength class and using safety coefficients.

4.2 Load Capacity of Tested Slab with Influence of Contact Surface

It was calculated with whole area of the slab in the previous chapter because in practice the real contact surface is not known. But the size of contact area can have very significant effect on the resulting behavior of foundation. The foundation slab can be completely rigid or completely flexible but it is neither one in practice. In practice the foundation slab is somewhere between rigid and flexible foundation. The above described will have different influence on distribution of stress into the foundation bottom. It has effect also on the punching resistance.

From the deformation measured on the described slab (Figs. 5, 6) approximate points where corners are up-lifted were calculated and from this point the real contact area was calculated in the last step of test. It was calculated on the safe side using simplified to linear course between the contact points. The resulting area is 3.52 m^2 and it is shown

Table 2 Maximum force in press according to the used value of strength.

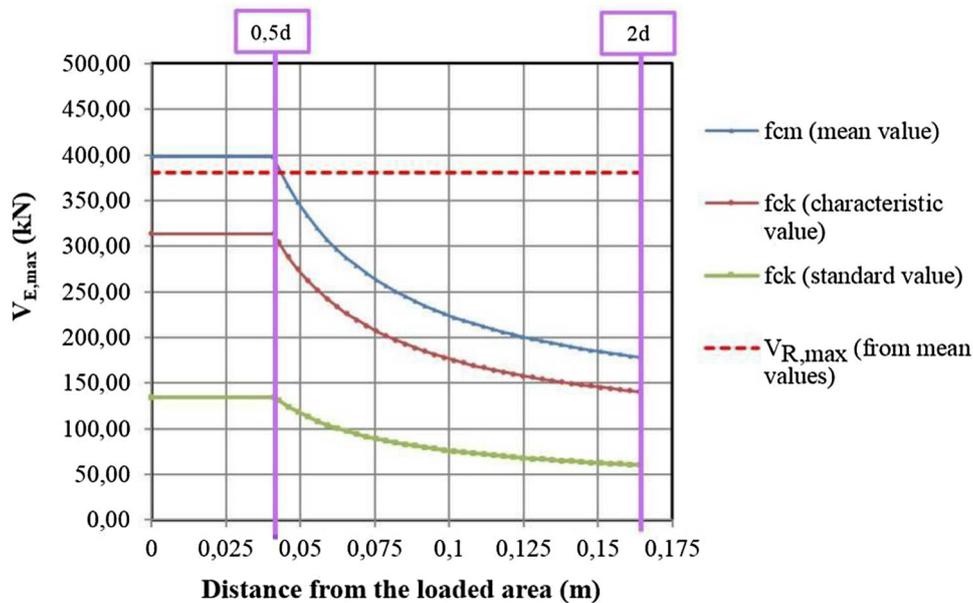| Maximum loading force depending on input parameters	Compressive cylinder strength (MPa)		Coefficient $C_{Rx,c}$		Coefficient γ_C	Maximal force (kN)
	Designation	Value (MPa)	Designation	Value (MPa)		
Mean values	f_{cm}	27.11	$C_{Rm,c}$	0.22	1.0	177.42
Characteristic values	f_{ck}	24.20	$C_{Rk,c}$	0.18	1.0	139.77
Standard values	f_{ck}	16.00	$C_{Rd,c}$	0.12	1.5	60.13

Fig. 10 Maximum punching shear force according to EC2.

on Fig. 11. If the shear resistance is calculated using this area, then the resulting bearing capacity will be more accurate—see Table 3. There are insignificant differences in comparison with Table 2 (about 1 kN).

But neither these results are accurate. Contact stress on the foundation bottom was measured at three points (centre, middle point of the edge and corner) and it is not uniform on the whole area of slab. From these measured data it is also clear that the corners were up-lifted.

4.3 Advanced Nolinear Analysis to Determine Total Load Capacity

The last and the main approach to the calculation of load capacity of concrete slab described in the present article is the advanced nonlinear analysis. This approach enables not only to determine the total load capacity but also to verify the structure collapse mode. The calculation is made in optional solutions for concrete and subsoil input parameters. The nonlinear analysis of concrete structures has been applied for many years ASCE (1982) and Barzegar (1988). Unfortunately, for a very long time the calculation solvers allowed

solving solely certain task types using bar or planar calculation models. The nonlinear analysis application was limited also by the knowledge of concrete material properties, demands for calculation and approaches in the model code.

The solution of the slab and subsoil task by numerical modelling was based on recommendations in Model Code 2010 (2012). The chosen constitutive concrete model is based on the fracture-plastic theory and 3D calculation model. ATENA calculation system is employed (Cervenka et al. 2007). The specific option is 3D Non Linear Cementitious 2 (Cervenka and Papanikolaou 2008). The determination of specific concrete parameters was also based on the recommendations in Sucharda and Konecny (2018) and Cervenka et al. (2007). The 3D calculation model comprises all major parts of the test setup of concrete slab with subsoil. The main components of the model are concrete slab, loading steel plate and subsoil. The finite element mesh has regular shape and consists of cubical elements. It is formed by a generator. The load is induced by force. The created calculation model is shown in Fig. 12 on the left. The modelled reinforcement is shown on Fig. 12 on the right.
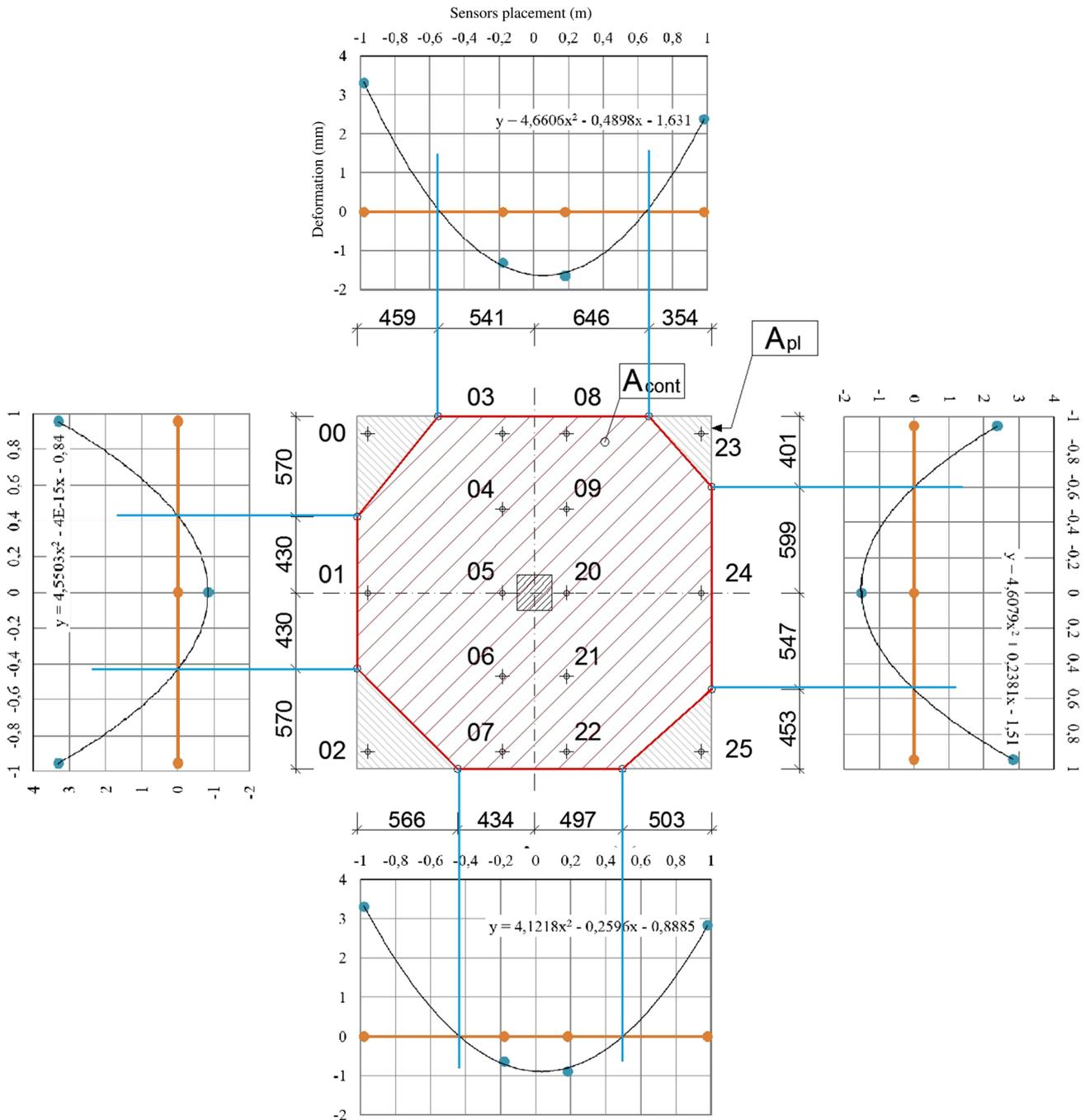
Fig. 11 Analysis of contact surface after step 5.

Table 3 Maximum force in press according to the used value of strength with the influence of contact surface.

Maximum loading force depending on input parameters	Compressive cylinder strength (MPa)		Coefficient $C_{Rx,c}$		Coefficient γ_C	Maximum force (kN)
	Designation	Value (MPa)	Designation	Value (MPa)		
Mean values	f_{cm}	27.11	$C_{Rm,c}$	0.22	1.0	178.42
Characteristic values	f_{ck}	24.20	$C_{Rk,c}$	0.18	1.0	140.55
Design values	f_{ck}	16.00	$C_{Rd,c}$	0.12	1.5	60.47

The obtained set of nonlinear equations is solved using the arc-length method. The solution of one option of the calculation task took 6–8 h. Following the nonlinear analysis the total load capacity and failure mode can be evaluated. Selected graphical results are provided in Fig. 13 for illustration. The achieved total slab load capacity for the different
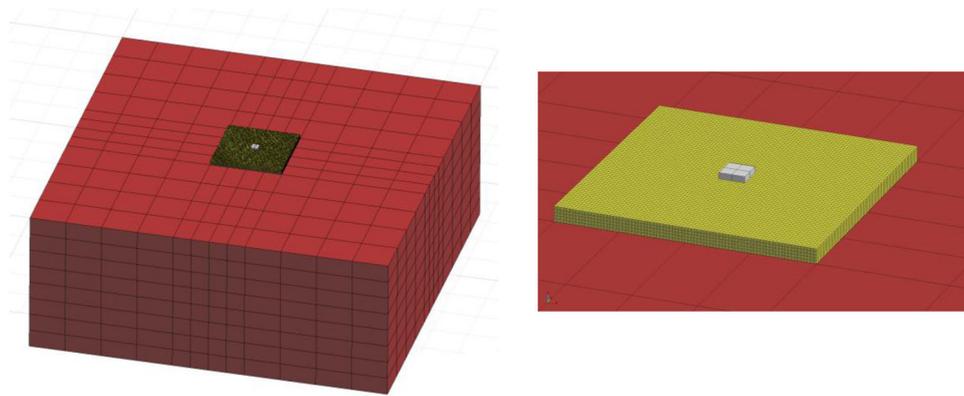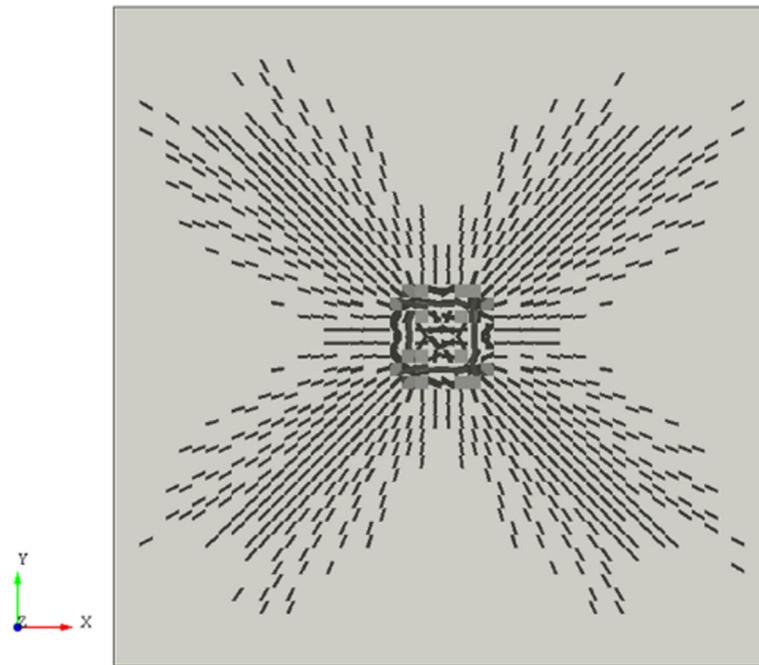
Fig. 12 3D Calculation model.

Fig. 13 Cracked slab: standard values for concrete and E_{def} 33.86 MPa.

Table 4 Maximum force in press according to the used value of strength with the nonlinear analysis.

Input value	Compressive cylinder strength	Tensile strength	Fracture energy	Modulus of elasticity of concrete	Modulus of elasticity of subsoil (MPa)	
					23.86	33.86
	F_{c} (MPa)	F_{t} (MPa)	G_{f} (N/m)	E_{c} (MPa)	Max. loading force (kN)	
Mean values	27.11	2.14	132	29,978	355.75	380.36
Characteristic values	24.20	1.92	130	28,865	357.39	357.75
Standard values	16.00	1.20	120	25,146	289.57	292.80

options is indicated in Table 4. Detailed analysis of the graphical results leads to a statement that the slab collapse mode is similar to that observed in the experiment. The concrete slab suffered punching shear failure. The crack development for 3D visualization just before the collapse can be seen in Fig. 14. The slab load capacity ranged between 289 and 380 kN. The maximum difference in the slab load capacity due to different subsoil load capacity was
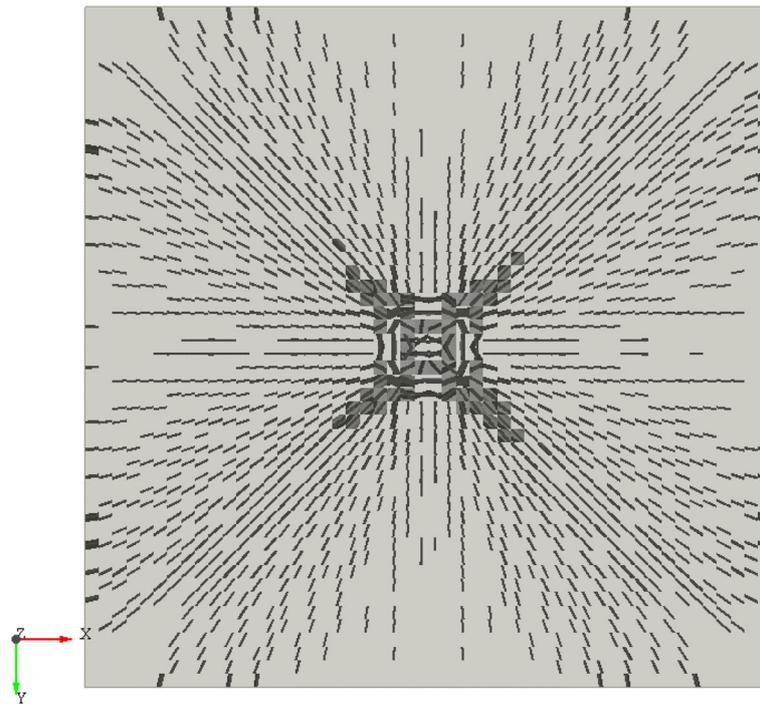
Fig. 14 3D cracked slab: standard values for concrete and E_{def} 33.86 MPa.

about 25 kN. The difference is more remarkable in case of input parameters for concrete in which case a difference up to 88 kN was observed.

5. Conclusion and Discussion

The article deals with research in the field of analysis of concrete slabs with low thickness exposed to high load in interaction with subsoil. Typically, the slabs form structures and floors in heavy industry and ground of aircraft taxiing areas. In these cases the typical approach to the concrete structure designing using verification models may not be optimal. The article and research presented comprise test of concrete slab followed by calculation of total load capacity in options based on existing design model code EC2 and nonlinear analysis using the finite element method.

The tested slab failed by punching shear at a force of 344 kN and an average distance of 1.7 d from the column perimeter, and the shape of the crack was an irregular oval. The irregular shape can be a result of inhomogeneous subsoil or also quicker progress of cracks on one side of the slab at higher load intensities. The test is documented in detail using record of deformation measurements. This is followed by detailed analysis of the slab failure for which purpose the slab was cut to eight pieces. The theoretical calculated value according to EC2 for the punching shear resistance was 60.13 kN, theoretical punching resistance based on mean values was 177.42 kN and it was located 2 d from the column perimeter. The real value of shear resistance is, as expected, larger than according to Eurocodes and the crack is in lower distance than according to Eurocodes. This means that Eurocodes are on the safe side.

In this case the real resistance was more than five times higher than the calculated value. However the foregoing facts confirm that the design punching shear resistance according to Eurocodes is very safe, maybe too safe. The approach using the calculation of load capacity of tested slab with influence of contact surface is also described. The application of verification models was followed by the advanced nonlinear analysis to determine the total load capacity. The analysis comprised application of 3D calculation model and fracture-plastic material. The use of created numerical model enabled a very good simulation of real behaviour of the slab. The calculated total slab load capacity for mean values was very similar to that observed in the experiment. The collapse mode was also covered very well in the numerical model. The differences between the experiment and numerical modelling results can be attributed to the spread and uncertainties in the input concrete and subsoil parameters. The slab load capacity ranged between 289 and 380 kN. The maximum difference in the slab load capacity due to different subsoil load capacity was about 25 kN. The difference is more remarkable in case of input parameters for concrete in which case a difference up to 88 kN was observed.

The use of relations for specific concrete properties described in Model Code 2010 (2012) proved useful. However, it should be noted that the calculations required by the nonlinear analysis are time and computationally consuming. The computational tasks were solved by 8 core processor with 64 GB of RAM memory typically 6–8 h. For numerical computations, it is so ideal to use HPC (High-performance computing). Because of that the nonlinear analysis is fit only in specific cases such as reconstructions and optimized designs where the use of typical verification

models would not be appropriate. It is also important to reflect the design and project criteria using, for example, global safety format, etc. in the nonlinear analysis.

Acknowledgement

Open Access

References

Aboutalebi, M., Alani, A., Rizzuto, J., & Beckett, D. (2014). Structural behaviour and deformation patterns in loaded plain concrete ground-supported slabs. *Structural Concrete, 15*(1), 81–93. https://doi.org/10.1002/suco.201300043.

Alani, A. M., & Beckett, D. (2013). Mechanical properties of a large scale synthetic fibre reinforced concrete ground slab. *Construction and Building Materials, 41,* 335–344. https://doi.org/10.1016/j.conbuildmat.2012.11.043.

ASCE. (1982). *Finite element analysis of reinforced concrete.* State of the Art Rep. No. 1982.

Barzegar, F. (1988). Layering of RC membrane and plate elements in nonlinear analysis. *Journal of the Struct. Div., 114*(11), 2474–2492.

Bazant, Z. P., Caner, F. C., Carol, I., Adley, M. D., & Akers, S. A. (2000). Microplane model M4 for concrete. I: Formulation with work-conjugate deviatoric stress. *Journal of Engineering Mechanics ASCE, 126*(9), 944–961.

Bazant, Z., & Planas, J. (1998). *Fracture and size effect in concrete and other quasibrittle materials.* Boca Raton: CRC Press.

Bogdándy, B., & Hegedűs, I. (2016). Determination of the punching cross-section of reinforced concrete flat slabs. *Periodica Polytechnica Civil Engineering., 60*(3), 405–411. https://doi.org/10.3311/ppci.8178.

Cajka, R. (2014). Comparison of the calculated and experimentally measured values of settlement and stress state of concrete slab on subsoil. *Applied Mechanics and Materials, 501,* 867–876.

Cervenka, V., Jendele, L., & Cervenka, J. (2007). *ATENA program documentation—part 1: Theory.* Pratur: Cervenka Consulting.

Cervenka, J., & Papanikolaou, V. K. (2008). Three dimensional combined fracture-plastic material model for concrete. *International Journal of Plasticity, 24*(12), 2192–2220. https://doi.org/10.1016/j.ijplas.2008.01.004.

EC2. (2006). ČSN EN 1992-1-1, Eurocode 2: Design of concrete structures—Part 1-1: General rules and rules for buildings.

Halvonik, J., & Fillo, L. (2013). The maximum punching shear resistance of flat slabs. *Procedia Engineering, 65,* 376–381.

Hegger, J., Ricker, M., Ulke, B., & Ziegler, M. (2007). Investigations on the punching behaviour of reinforced concrete footings. *Engineering Structures, 29,* 2233–2241. https://doi.org/10.1016/j.engstruct.2006.11.012.

Hegger, J., Sherif, G. A., & Ricker, M. (2006). Experimental investigations on punching behavior of reinforced concrete footings. *ACI Structural Journal, 103,* 604–613.

Hoang, L. C., & Pop, A. (2016). Punching shear capacity of reinforced concrete slabs with headed shear studs. *Magazine of Concrete, 68*(3), 118–126.

Husain, M., Eisa, A. S., & Roshdy, R. (2017). Alternatives to enhance flat slab ductility. *International Journal of Concrete Structures and Materials, 11*(1), 161–169. https://doi.org/10.1007/s40069-016-0180-5.

Ibrahim, M., & Metwally, I. M. (2014). Three-dimensional finite element analysis of reinforced concrete slabs strengthened with epoxy-bonded steel plates. *Advances in Concrete Construction, 2*(2), 91–108. https://doi.org/10.12989/acc.2014.2.2.091.

ISO. (1998). General principles on reliability for structures, ISO 2394.

JCSS. (2016). Probabilistic model code. JCSS Working Material. http://www.jcss.ethz.ch/.

Kolář, V., & Němec, I. (1989). *Modelling of soil-structure interaction.* New York: Elsevier. ISBN 04-449-8859-9.

Kotsovou, M. G., Kotsovos, M. G., & Vougioukas, E. (2016). Assessment of design methods for punching through numerical experiments. *Computers and Concrete, 17*(3), 305–322. https://doi.org/10.12989/cac.2016.17.3.305.

Kueres, D., Siburg, C., Herbrand, M., Classen, M., & Hegger, J. (2017). Uniform design method for punching shear in flat slabs and column bases. *Engineering Structures, 136*(1), 149–164. https://doi.org/10.1016/j.engstruct.2016.12.064.

Lahuta, H., Hrubesova, E., Duris, L., & Petrasova, T. (2015). Behaviour subsoil of slab foundation under loading. *International Multidisciplinary Scientific GeoConference Surveying Geology and Mining Ecology Management, 2*(1), 119–126.

Model Code 1990. (1993). Final draft, fib, Bulletin

Model Code 2010. (2012). Final draft, fib, Bulletin no. 65 and 66, 1–2

Norm ACI 318-08. (2008). Building code requirements for structural concrete (ACI 318-08) and commentary (ACI 318-08)

Norm SIA 262. (2003). April 2003. Betonbau—Schweizer Norm SN 505 262

Ricker, M., & Siburg, C. (2016). Punching shear strength of flat slabs—critical review of Eurocode 2 and fib Model Code 2010 design provisions. *Structural Concrete, 17*(3), 457–468.

Sarfarazi, V., et al. (2016). A new approach for measurement of tensile strength of concrete. *Periodica Polytechnica Civil Engineering., 60*(2), 199–203. https://doi.org/10.3311/PPci.8328.

Siburg, C., Häusler, F., & Hegger, J. (2012). Flat slab punching design according to German annex of Eurocode 2 [Durchstanzen von flachdecken nach NA(D) zu Eurocode 2]. *Bauingenieur, 8*(5), 216–225.

Siburg, C., & Hegger, J. (2014). Experimental investigations on the punching behaviour of reinforced concrete footings with structural dimensions. *Structural Concrete, 15*(3), 331–339. https://doi.org/10.1002/suco.201300083.

Siburg, C., Ricker, M., & Hegger, J. (2014). Punching shear design of footings: critical review of different code provisions. *Structural Concrete., 15*(4), 497–508. https://doi.org/10.1002/suco.201300092.

Song, J.-K., Kim, J., Song, H.-B., & Song, J.-W. (2012). Effective punching shear and moment capacity of flat plate-column connection with shear reinforcements for lateral loading. *International Journal of Concrete Structures and Materials, 6*(1), 19–29. https://doi.org/10.1007/s40069-012-0002-3.

Sucharda, O., & Konecny, P. (2018). Recommendation for the modelling of 3D non-linear analysis of RC beam tests. *Computers and Concrete, 21*(1), 11–20. https://doi.org/10.12989/cac.2018.21.1.011.

Sucharda, O., Pajak, M., Ponikiewski, T., & Konecny, P. (2017). Identification of mechanical and fracture properties of self-compacting concrete beams with different types of steel fibres using inverse analysis. *Construction and Building Materials, 138,* 263–275. https://doi.org/10.1016/j.conbuildmat.2017.01.077.

Vecchio, F. J., & Shim, W. (2004). Experimental and analytical reexamination of classic concrete beam tests. *Journal of Structural Engineering., 130*(3), 460–469.

Zabulionis, D., Sakinis, D., & Vainiunas, P. (2006). Statistical analysis of design codes calculation methods for punching sheer resistance in column-to-slab connections. *Journal of Civil Engineering and Management, 12,* 205–213. https://doi.org/10.1080/13923730.2006.9636394.